Focusing adaptive-optics for neutron spectroscopy at extreme conditions

Cite as: Appl. Phys. Lett. **107**, 243503 (2015); https://doi.org/10.1063/1.4938071
Submitted: 09 September 2015 • Accepted: 04 December 2015 • Published Online: 15 December 2015

G. G. Simeoni, R. G. Valicu, G. Borchert, et al.

Focusing adaptive-optics for neutron spectroscopy at extreme conditions

G. G. Simeoni,[1,2,a)] R. G. Valicu,[1,2,3] G. Borchert,[1] P. Böni,[3] N. G. Rasmussen,[4] F. Yang,[5] T. Kordel,[5] D. Holland-Moritz,[5] F. Kargl,[5] and A. Meyer[5]
[1]*Heinz Maier-Leibnitz Zentrum (MLZ), FRM II, Technical University of Munich, D-85748 Garching, Germany*
[2]*Physics Department E13, Technical University of Munich, D-85748 Garching, Germany*
[3]*Physics Department E21, Technical University of Munich, D-85748 Garching, Germany*
[4]*Nanoscience Center, Niels Bohr Institute, University of Copenhagen, Universitetsparken 5, DK-2100 Copenhagen, Denmark*
[5]*Institut für Materialphysik im Weltraum, Deutsches Zentrum für Luft- und Raumfahrt, D-51170 Köln, Germany*

(Received 9 September 2015; accepted 4 December 2015; published online 15 December 2015)

Neutron Spectroscopy employing extreme-conditions sample environments is nowadays a crucial tool for the understanding of fundamental scientific questions as well as for the investigation of materials and chemical-physical properties. For all these kinds of studies, an increased neutron flux over a small sample area is needed. The prototype of a focusing neutron guide component, developed and produced completely at the neutron source FRM II in Garching (Germany), has been installed at the time-of-flight (TOF) disc-chopper neutron spectrometer TOFTOF and came into routine-operation. The design is based on the *compressed Archimedes' mirror* concept for finite-size divergent sources. It represents a unique device combining the supermirror technology with Adaptive Optics, suitable for broad-bandwidth thermal-cold TOF neutron spectroscopy (here optimized for 1.4–10 Å). It is able to squeeze the beam cross section down to a square centimeter, with a more than doubled signal-to-background ratio, increased efficiency at high scattering angles, and improved symmetry of the elastic resolution function. We present a comparison between the simulated and measured beam cross sections, as well as the performance of the instrument within real experiments. This work intends to show the unprecedented opportunities achievable at already existing instruments, along with useful guidelines for the design and construction of next-generation neutron spectrometers. © *2015 AIP Publishing LLC*.
[http://dx.doi.org/10.1063/1.4938071]

Neutrons have a mass and are chargeless, 1/2-spin particles, i.e., neutral probes that interact directly with the nuclei, unpaired electrons, and magnetic moments. The typical kinetic energies of cold neutrons of a few meV naturally match the energy scale of atomic and molecular vibrations. Moreover, neutrons are sensitive to isotopic substitution.[1]

For the above-mentioned reasons and notwithstanding the intrinsic low brilliance of the neutron sources when compared to synchrotrons and laser facilities, neutron scattering currently experiences an increasing interest. This is embodied in the construction of the European Spallation Source (ESS) in Lund (Sweden).[2] Relevant for the present work, the high penetrating power of the neutron beam allows the employment of massive sample environments without the need for optical access to the sample, which traditionally encountered the interest of geophysics, planetary physics, oceanography, and aerospace applications. Nowadays, there is a wide range of additional emergent scientific investigations, naturally seeking for extreme sample environments: molecular magnetism, quantum criticality, multiferroics, *ab-melting* design of liquid metals and alloys, fuel elements for aircrafts and rockets, survivability, and adaptation of extremophile bacteria.[3–9] The common issue is that extreme-conditions set-ups require samples smaller than usual, due to intrinsic technical, availability, and safety reasons.[10–12] Therefore, the list can be merged together with that of limited-availability samples like biological materials or single crystals.[13–15]

We developed a compact focusing device for TOFTOF,[16] with design based on the *compressed Archimedes' mirror* for finite-size divergent sources proposed by Simeoni.[17] TOFTOF is a thermal-cold (1.4–14 Å) neutron chopper time-of-flight (TOF) spectrometer installed at the FRM II in Garching (Germany). Besides its excellent flexibility (elastic, quasi-elastic, and inelastic scattering), its traditional linearly tapered ballistic neutron guide with increasing supermirror coating (m = 2–3.5) represents an intermediate stage in the evolution from the earlier straight guides towards the modern fully ballistic elliptic guides.[18–22]

This development phase completed the global conceptual upgrade of TOFTOF for extreme-conditions investigations. We preserved the traditional configuration as option and introduced the possibility to switch a compact focusing device into the beam, thus replacing the last 500 mm of the guide system. This corresponds to less than 5% of the instrument length and less than 1% of the total neutron path from the source to the sample. The adjustable curvature of the device (Adaptive-Optics technology) sets the optical focal point (flux density maximum) at the sample position upon varying the incoming neutron wavelength.

The design took into account both the signal-to-background ratio and the neutron statistics. The first one is relevant for neutron scattering in general, whereas the second one is more crucial for spectroscopy, since the energy-resolved data acquisition leads to signal intensities of typical four orders of magnitude lower than comparable diffraction experiments. The simultaneous optimization of the two figures of Merit (FoM) is non-trivial: the neutron statistics benefits from a higher neutron flux at the sample position, but the

a)Author to whom correspondence should be addressed. Electronic mail: ggsimeoni@outlook.com

signal-to-background ratio would be unaffected by a bare increase of the neutron flux. Only a more efficient sample illumination could improve the latter, e.g., upon reducing or even eliminating any scattering from the sample environment.

In this letter, we discuss the short and middle term scientific perspectives of this and similar spectrometers. Our solution fits the requirements of a finite-size neutron source, where pure shading optics (slits or pinholes) would downgrade the instrument and truly focusing optics (point-like source) does not apply. For the long-term perspectives, calculations allowing a deeper conceptual revision have been carried out and reported elsewhere.[23] These are in fair agreement with some general guidelines for much longer focusing ballistic systems,[24–30] and complementary to the *Selene concept*.[31–33]

The focusing neutron optics experienced huge technological development over the last years.[34,35] Compact global solutions for broad-bandwidth thermal-cold TOF neutron spectroscopy have been only marginally addressed though.

The neutron transport exploits the Bragg total reflection from artificial multilayers (*supermirror* coating), just like the reflective X-ray optics, and allows complex optical systems, in analogy to visible-light optics.[36] At a macroscopic level, the ensemble of supermirrors (e.g., a ballistic guide) might behave as an extended but single object that transmits and transforms the beam: namely, a lens.

The monochromatic focal length of a conventional lens depends on the convexity of the refractive surfaces; the monochromatic focal length of a neutron lens depends on the curvature of the reflecting surfaces. The chromatic transmission of a visible-light lens is ruled by the refractive index $n(\lambda)$; the chromatic transmission of a neutron lens is ruled by the critical angle $\theta_c(\lambda)$ and the corresponding divergence distribution of the accepted/reflected trajectories.

The definitions of geometrical *focus* and optical *focal point* are distinct and independent. The ambiguity with visible-light beams derives from Latin language using the same word "focus" for both properties, with a *post-litteram* definition confusing centuries of studies by the Ancient Greeks with modern concepts in a very simplistic way.

Concepts like magnification, field depth, etc., apply to neutron optics systems too, along with the whole set of aberrations.[35,37] In the case of direct-geometry neutron spectroscopy, it is the chromatic aberration. Various independent aspects are contained in works carried out by Böni,[25] Bentley,[37,38] and Stahn,[31,32] with markedly wavelength-dependent optimization results. However, the issue has been debated mostly in terms of divergence and brilliance so far, and no real investigation of the focal displacement in real situations. A rationale for the chromatic aberration has been developed by Simeoni.[17]

The basic of any ballistic focusing is the increased beam divergence of the reflected neutron trajectories (*neutron rays* in the computer simulations), which converge in the neighborhood of the focal point $\mathbf{F_{out}}$.

Differently from the ideal case, we observe that in fact:

(1) The source is not point-like.
(2) The supermirror coating, whilst increasing the critical angle, introduces a wavelength-dependent upper cutoff $\theta_c(\lambda)$ to the numerical aperture.

As an effect, the intersection of the convergent trajectories is weighted by a wavelength-dependent divergence distribution. At fixed curvature, the longer the wavelength, the higher the average divergence, the closer $\mathbf{F_{out}}(\lambda)$ to the exit of the guide.[17,26]

Direct-geometry neutron spectrometers like TOFTOF do not support the insertion of pinholes, and too high supermirror coatings would destroy the inelastic resolution (especially for single crystals). Indeed, the choppers and the neutron guide are mutually optimized along their entire length (10 m) and match the resolution of the detectors. In general, a feasible upgrade is easily compatible only with the integration of a single, tunable device. This prevents, e.g., the use of poly-capillary,[15] multichannel,[38] or nested Kirckpatrick-Baez neutron guides,[39,40] as well as the solutions for triple-axis spectrometers.[24,41,42]

We installed the focusing device in the *exchange guide*. This is a box hosting two switchable guide stages, sharing the vacuum system with the rest of the primary spectrometer (Fig. 1(a)). The very limited size of the vacuum vessel would have never allowed the installation of commercial Adaptive-Optics. Thanks to the synergy of computer simulations, laboratory tests, and neutron measurements, the design and the production of the device took place completely at the FRM II. It is compatible with the oscillating radial collimator. The supermirror coating $m = 3.5$ is the same of the replaced guide segment, thus preserving elastic and inelastic energy resolution.[23]

Main features of the prototype: variable rectangular cross section; four independent supermirror walls, whose bending concept is illustrated in Fig. 1(c). The combination of elastic elongation and bending leads to a parabolic curvature. As shown in Fig. 1(a), the vertical/horizontal wall-to-wall distance at the entrance (***H***) and the exit (***h***) of the device identify the supermirror curvature. ***H*** is fixed and chosen in order to accept the full divergence of the previous guide segment, whereas the piezoactuators tune ***h*** according to an optimized bending

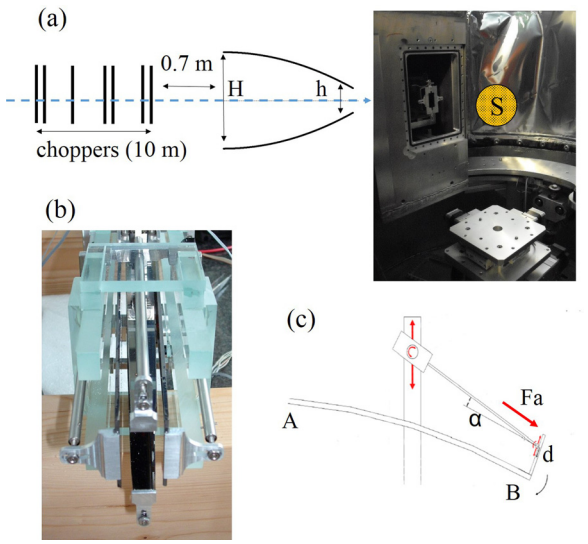

FIG. 1. (a) TOFTOF scheme, with scale emphasizing the focusing device terminating in the flight chamber. The picture shows the sample position "S" without sample environment and radial collimator. (b) Front view of the prototype. We recognize the 4 rods pressing the supermirrors, and the external glass casing hosting the body of the piezomotors. (c) The bending concept. The extremity A is fixed whereas the extremity B, close to the sample, is moved by a piezomotor. The latter, via an Al rod, presses a small vertical Al plate of length *d* and behaves as lever on the supermirror. The motor body can rotate around its transverse axis, preventing any blocking at the maximal curvature.

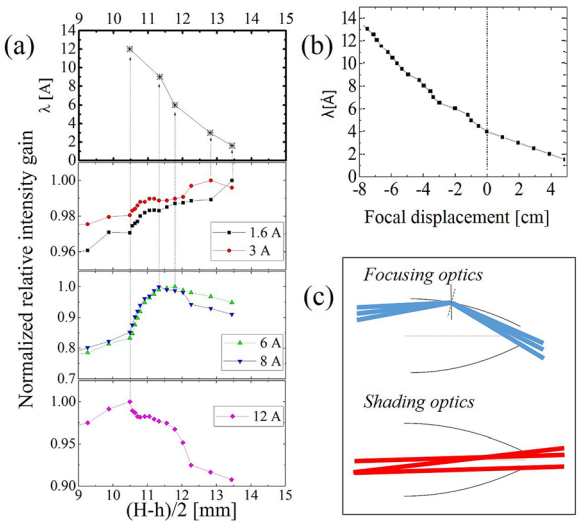

FIG. 2. (a) Sensitivity of the elastic scattering to a curvature change of the vertical supermirror reflectors (H fixed, h variable). Intensities normalized to 1 at the maximum, disregarding the absolute comparison with the standard configuration. (b) Wavelength-dependent displacement of the focal point with a 500 m-long elliptic nose optimized for 4 Å (McStas Simulations); (c) comparison between focusing optics (blue trajectories) and shading optics (red trajectories).

algorithm. Monte-Carlo ray tracing simulations (McStas package[43]) delivered the optimized values of $\boldsymbol{h}$. Opto-mechanical laboratory tests converted $\boldsymbol{h}$ in piezomotor settings, thus including all necessary gravitational corrections. Detailed information is contained in the supplementary material.[44]

We quantified the impact of the chromatic aberration: the curvature-dependent focal displacement at fixed wavelength (Fig. 2(a)) and the wavelength-dependent focal displacement at fixed curvature (Fig. 2(b)). Both plots show the same non-linear behaviour, mimicking the non-linear behaviour of $\theta_c(\lambda)$. Fig. 2(a) is based on elastic scattering experiments from a Vanadium reference sample, looking for the curvature maximizing the neutron flux over 1 cm^2. The value varies between the optimal settings for 1.4 Å (maximal curvature) and those ones for 14 Å (minimal curvature). Three distinct regimes are distinguishable: (i) $\lambda < 4$ Å (optimal settings close to the maximal curvature); (ii) 4 Å $< \lambda <$ 10 Å (pronounced maximum and marked sensitivity to a curvature change); and (iii) $\lambda > 10$ Å (maximum accompanied by a broad intensity plateau). This plateau accompanies the experimentally measured change of convexity at the longest wavelengths (Fig. 2(a)—top) and will be discussed below. In Fig. 2(b), McStas simulations of an elliptical nose (archetypal ballistic guide), replacing the traditional linearly tapered segment, lead to a focal point moving by several centimeters.[45] This clearly affects both thermal and cold neutrons at the same order. Relevant is the ability of our device to keep the focal point at the sample position at any wavelength of interest. The complete optimization procedure is described in detail in the supplementary material.[44] Fig. 2(c) points out two distinct classes of neutron trajectories: (i) reflected trajectories (focused component) and (ii) non-interacting trajectories (divergent component, *shading optics*). The argument of the chromatic aberration applies only to the focused, convergent component.

The instrumental performance has been characterized by neutron imaging, elastic scattering from a reference sample, and inelastic scattering experiments with extreme-conditions set-ups.

Neutron imaging in Fig. 3(a) highlights the distinct compromise between focusing and shading optics in the thermal and the cold regime, as signal-to-background ratio counterpart of the distinct regimes outlined in Fig. 2(a). Fig. 3(b) shows the excellent agreement between McStas simulations and neutron imaging at 3 Å.[23]

Vanadium is a typical calibration reference. We collected the elastic scattering from a cylindrical sample (1×1 cm^2 cross section) with the same guide configurations used for neutron imaging. We fitted the elastic line with a Gaussian function and a flat background.

The intensity gain ranges between +30% and +100% (Fig. 4(a)). The values are validated by several inelastic scattering measurements with extreme-conditions equipments[46–52] (see Fig. 4(a)-inset for the electrostatic levitator[46,47]) and, in the cold region, overlap the prediction of Bentley with a set of optimized 0.5 m-long parabolic guides for IN5 at the Institut Laue-Langevin (ILL) in Grenoble (France).[38]

We set at 10 Å the limit of operation of our device, in agreement with Fig. 2(a). Longer wavelengths experience,

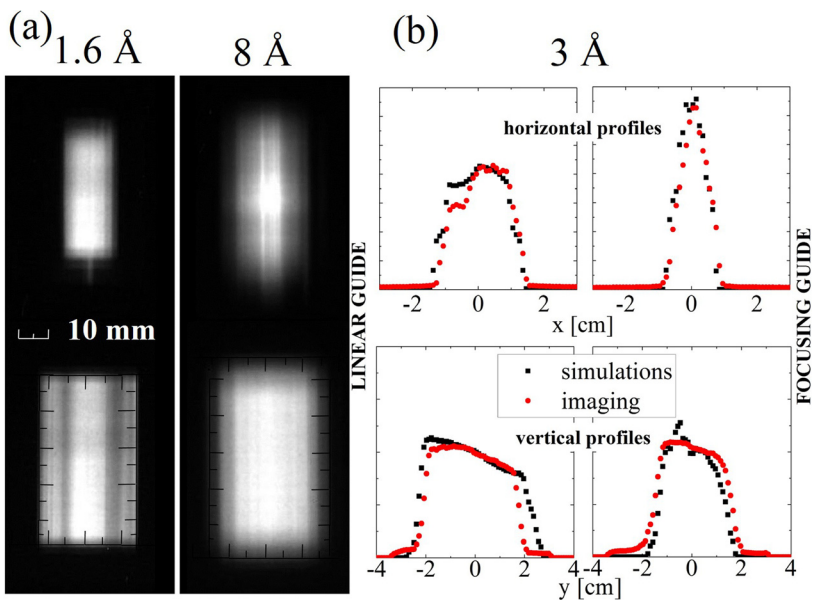

FIG. 3. (a) Neutron imaging at 1.6 Å and 8 Å, with (top) and without (bottom) the focusing device. Pictures taken with a neutron sensitive CCD camera, i.e., a 6LiF/ZnS scintillator. (b) Comparison between McStas simulations and data from neutron imaging at 3 Å, with the linearly tapered guide (left) and the focusing device (right), along the horizontal direction (top) and the vertical direction (down).

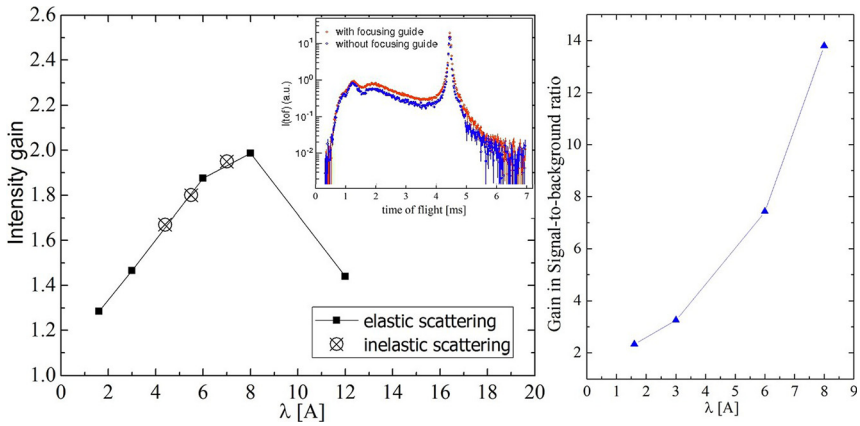

FIG. 4. (a) Intensity gain from elastic and inelastic scattering—inset: inelastic scattering at 4.4 Å, with and without focusing device, from 0.5 g (6 mm diameter) Vitreloy (ZrTiNiCuBe) samples under electrostatic levitation at 1110 K.[46,47] (b) Gain in signal-to-background ratio as measured with a Vanadium sample with a size of $1 \times 1\,cm^2$. The gain is normalized to 1 for the linearly tapered guide.

namely, low focusing efficiency (Fig. 4(a)), almost unvaried background area (neutron imaging), and low sensitivity to curvature changes (Fig. 2(a)). Moreover, the neutron flux for $\lambda > 10$ Å is already very small. The neutrons are redistributed within the same area, with only setup-dependent gain in signal-to-background ratio. This is apparently a surprising finding, since longer wavelengths are believed to focalize better. We should rather consider that, with respect to the guide exit, the non-linear tapering tendentially causes short wavelengths underfocusing and long wavelengths overfocusing (Fig. 2(b)). Being intrinsically difficult to defocus with any focusing geometry, long wavelengths can require systems extending even inside the sample environment.[53] Conversely, at short wavelengths, it would be sufficient to stop the reflections far away from the sample. Differently from typical approaches optimized for cold neutrons, we optimized the device for thermal neutrons relaxing the curvature for the cold ones. Above 10 Å, the device is almost straight. The excellent optical magnification in the focal plane is due to the *compressed Archimedes' mirror* concept, exploiting the parabolic properties for non ideal sources.[17]

The signal-to-background ratio from $1 \times 1\,cm^2$ samples ranges between 6×10^3 (1.6 Å) and 4×10^4 (8 Å). The gain factor with respect to the linearly tapered geometry, varying between 2 and 14, shows the reached feasibility of extreme-conditions experiments (Fig. 4(b)). The ratio has been defined according to Fig. 5(a). The reference values measured with the linearly tapered geometry over $1 \times 1\,cm^2$ correspond to one tenth of those ones reported in the previous TOFTOF literature,[16] where the instrument was traditionally calibrated for sample areas of $2.5 \times 4\,cm^2$: one tenth of sample area (illuminated by the same big cross section) generates one tenth of sample signal. After Fig. 4(b), one can also consider the convenience of employing small samples with the focusing device in spite of much bigger samples with the linearly tapered guide, independently from the used sample environment. Indeed, rescaling the results in the other direction (i.e., from small to big area), a gain factor of 10 over $1\,cm^2$ can be interpreted as a small sample in the focusing geometry performing like a ten times bigger sample in the standard linearly tapered configuration. At 8 Å, e.g., the focusing device is more convenient also for standard experiments. For the intermediate case of 6 Å, we deduce: (i) feasibility, as the prototype enhances the ratio by a factor 7 (2.2×10^4 vs. 3×10^3) over $1\,cm^2$; (ii) convenience, as a tenth of sample with the focusing device almost compares to large samples[16] (2.2×10^4 vs. 3×10^4, respectively). Extremely relevant for quasi-elastic experiments, the elastic resolution is conserved and the wings' asymmetry removed (Fig. 5(b)).

The prototype came already into routine-operation with disparate set-ups and samples. In several studies, the improved statistics simplifies the otherwise tough (and tedious) discrimination of the empty can contribution. In general, quasi-elastic investigations benefit now from faster acquisition times and data with qualitatively higher content of scientific information: improved elastic resolution, negligible multiple scattering corrections, enlarged useful low-Q range, and depleted phononic cell-background. On its turn, the inelastic scattering takes enormous advantage of the lowered set-up illumination, and the *inter alia* reduced nuclear activation. Among the already performed experiments, we mention those employing the electrostatic levitator,[46–49] the high-temperature vacuum furnace,[50,51] and Paris-Edinburgh cells[52] (intensity gains in Fig. 4(a)).

We developed a unique, compact Adaptive-Optics device suitable for thermal-cold TOF neutron spectroscopy with small

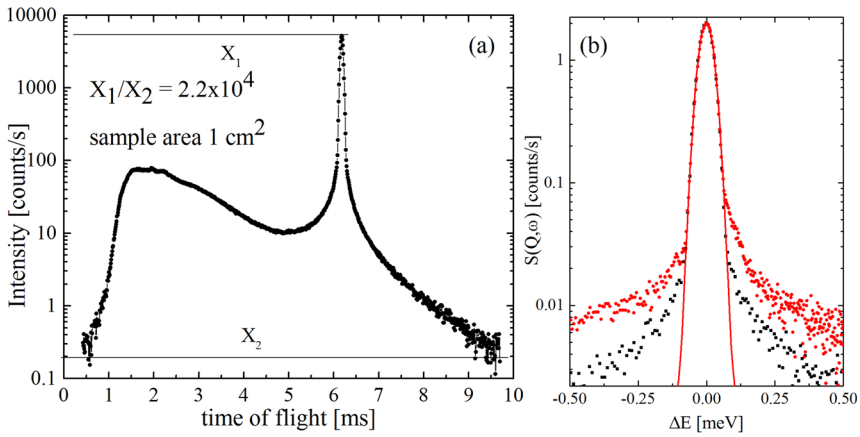

FIG. 5. Scattered intensity from reference Vanadium samples at 6 Å, 12 000 rpm, ratio 4. (a) Inelastic scattering and definition of the signal-to-background ratio from $1\,cm^2$ sample area with the focusing device; (b) elastic scattering from $1\,cm^2$ sample area with the focusing device (black full squares), elastic scattering from $10\,cm^2$ sample area with the standard linearly tapered guide (red full circles), and elastic resolution (straight line).

samples (1 cm^2). While preserving the traditional instrumental configuration as option, the prototype introduces the advantages of a non-linearly focusing geometry also into a linearly tapered guide system. The control on the focal point is achieved via the adjustable curvature of the supermirrors, overcoming the technical impossibility of employing divergence limiters or beam stoppers at TOF spectrometers. Such result relies on two pillars: (1) primary optimization for the thermal neutrons, not the cold ones; (2) dedicated design for finite-size divergent sources, disregarding the ideal approximations (*compressed Archimedes' mirror* concept[17]). Due to its complementarity, our solution represents a valid alternative to the *Selene* concept.[31,32] This compact device (less than 1% of the total source-sample distance) combines a high focusing efficiency (between +30% and +100% increase in signal intensity) with a markedly enhanced signal-to-background ratio. Thanks to the higher symmetry of the elastic resolution, quasi-elastic experiments experience also a qualitative improvement. Altogether, the significant impact on both inelastic and quasi-elastic scattering paves the way for pioneering scientific projects. After dedicated calibration, the design applies to ballistic guides in general and is suited for TOF spectrometers, triple-axis, and diffractometers.

G.G.S. acknowledges K. Lefmann for fruitful discussion and constructive criticism. G.G.S., R.G.V., and G.B. are grateful to J. Weber, E. Kahle, and the FRM II Neutron Optics Group for technical assistance during the assembly and the installation of the device. This work received the financial support of the Seventh Framework Program of the European Union via the NMI3-Project 226507 "*Adaptive optics for extreme environments*."

[1]L. Liang, R. Rinaldi, and H. Schober, *Neutron Application in Earth, Energy and Environmental Science* (Springer, 2009).
[2]See www.docdb01.ess.lu.se/DocDB/0002/000274/015/TDR_online_ver_all.pdf for ESS Technical Design Report, 2013.
[3]M. L. Baker, T. Guidi, S. Carretta, J. Ollivier, H. Mutka, H. U. Güdel, G. A. Timco, E. J. L. McInnes, G. Amoretti, R. E. P. Winpenny, and P. Santini, Nat. Phys. **8**, 906 (2012).
[4]A. B. Boeer, A.-L. Barra, L. F. Chibotaru, D. Collison, E. J. L. McInnes, R. A. Mole, G. G. Simeoni, G. A. Timco, L. Ungur, T. Unruh, and R. E. P. Winpenny, Angew. Chem., Int. Ed. **50**, 4007 (2011).
[5]S. Mühlbauer, B. Binz, F. Jonietz, C. Pfleiderer, A. Rosch, A. Neubauer, R. Georgii, and P. Böni, Science **323**, 915 (2009).
[6]R. Ritz, M. Halder, M. Wagner, C. Franz, A. Bauer, and C. Pfleiderer, Nature **497**, 231 (2013).
[7]A. Meyer, EPJ Web Conf. **83**, 01002 (2015).
[8]F. Meersman and P. F. McMillan, Chem. Commun. **50**, 766 (2014).
[9]A. Picard and I. Daniel, Biophys. Chem. **183**, 30 (2013).
[10]I. Goncharenko, I. Mirebeau, P. Molina, and P. Böni, Phys. B: Condens. Matter **234–236**, 1047 (1997).
[11]S. Klotz, Th. Strässle, G. Rousse, G. Hamel, and V. Pomjakushin, Appl. Phys. Lett. **86**, 031917 (2005).
[12]S. Klotz, M. Braden, and J. M. Besson, Hyperfine Interact. **128**, 245 (2000).
[13]F. Foglia, R. Hazael, G. G. Simeoni, M.-S. Appavou, M. Moulin, M. Haertlein, T. Forsyth, T. Seydel, I. Daniel, F. Meersman, and P. F. McMillan, "Water dynamics in Shewanella Oneidensis at ambient and high pressure using quasi-elastic neutron scattering," Sci. Rep. **5**, 18862 (2015).
[14]M.-S. Appavou, S. Busch, W. Doster, A. Gaspar, and T. Unruh, Eur. Biophys. J. **40**, 705 (2011).
[15]W. M. Gibson, A. J. Schultz, H. H. Chen-Mayer, D. F. R. Mildner, T. Gnäupel-Herold, M. E. Miller, H. J. Prask, R. Vitt, R. Youngman, and J. M. Carpenter, J. Appl. Crystallogr. **35**, 677 (2002).
[16]T. Unruh, J. Neuhaus, and W. Petry, Nucl. Instrum. Methods A **580**, 1414 (2007).
[17]G. G. Simeoni, "A non-imaging focusing concept for finite-size divergent neutron, light and sound sources: adjustable compressed Archimedes' mirror," J. Opt. (submitted).
[18]S. Roth, A. Zirkel, J. Neuhaus, W. Schneider, and W. Petry, Physica B **283**, 439 (2000).
[19]A. Zirkel, S. Roth, W. Schneider, J. Neuhaus, and W. Petry, Physica B **276–278**, 120 (2000).
[20]M. Yonemura, K. Mori, T. Kamiyama, T. Fukunaga, S. Torii, M. Nagao, Y. Ishikawa, Y. Onodera, D. S. Adipranoto, H. Arai, Y. Uchimoto, and Z. Ogumi, J. Phys.: Conf. Ser. **502**, 012053 (2014).
[21]H. Arima, K. Komatsu, K. Ikeda, K. Hirota, and H. Kagi, Nucl. Instrum. Methods A **600**, 71 (2009).
[22]R. M. Ibberson, Nucl. Instrum. Methods A **600**, 47 (2009).
[23]N. G. Rasmussen, G. G. Simeoni, and K. Lefmann, "Optimizing a neutron-beam focusing device for the direct geometry time-of-flight soectrometer TOFTOF at the FRM II research reactor," Nucl. Instrum. Methods A (submitted).
[24]S. Mühlbauer, P. G. Niklowitz, M. Stadlbauer, R. Georgii, P. Link, J. Stahn, and P. Böni, Nucl. Instrum. Methods A **586**, 77 (2008).
[25]P. Böni, Nucl. Instrum. Methods A **586**, 1 (2008).
[26]C. Schanzer, P. Böni, U. Filges, and T. Hils, Nucl. Instrum. Methods A **529**, 63 (2004).
[27]T. Hils, P. Böni, and J. Stahn, Physica B **350**, 166 (2004).
[28]H. Jacobsen, K. Lieutenant, C. Zendler, and K. Lefmann, Nucl. Instrum. Methods A **717**, 69 (2013).
[29]M. Bertelsen, H. Jacobsen, U. B. Hansen, H. H. Carlsen, and K. Lefmann, Nucl. Instrum. Methods A **729**, 387 (2013).
[30]K. H. Klenø, K. Lieutenant, K. H. Andersen, and K. Lefmann, Nucl. Instrum. Methods A **696**, 75 (2012).
[31]J. Stahn, T. Panzner, U. Filges, C. Marcelot, and P. Böni, Nucl. Instrum. Methods A **634**, S12 (2011).
[32]J. Stahn, U. Filges, and T. Panzner, Eur. Phys. J. Appl. Phys. **58**, 11001 (2012).
[33]E. Hüger, J. Stahn, and H. Schmidt, J. Electrochem. Soc. **162**, A7104 (2015).
[34]H. Wolter, Ann. Phys. **445**, 94 (1952); **445**, 286 (1952).
[35]F. Ott, *Modern Developments in X-ray and Neutron Optics*, Springer Series in Optical Science Vol. 137, edited by A. Erko, M. Idir, Th. Krist, and A. G. Michette (Springer, 2008), pp. 113–134.
[36]G. E. Ice, J. D. Budai, and J. W. L. Pang, Science **334**, 1234 (2011).
[37]P. M. Bentley, S. J. Kennedy, K. H. Andersen, D. Martin Rodriguez, and D. F. R. Mildner, Nucl. Instrum. Methods A **693**, 268 (2012).
[38]P. M. Bentley and K. H. Andersen, J. Appl. Cryst. **42**, 217 (2009).
[39]G. E. Ice, J.-Y. Choi, P. Z. Takacs, A. Khounsary, Y. Puzyrev, J. J. Molaison, C. A. Tulk, K. H. Andersen, and T. Bigault, Appl. Phys. A **99**, 635 (2010).
[40]G. E. Ice, C. R. Hubbard, B. C. Larson, J. W. L. Pang, J. D. Budai, S. Spooner, and S. C. Vogel, Nucl. Instrum. Methods A **539**, 312 (2005).
[41]M. Janoschek, P. Böni, and M. Braden, Nucl. Instrum. Methods A **613**, 119 (2010).
[42]T. Adams, G. Brandl, A. Chacon, J. N. Wagner, M. Rahm, S. Mühlbauer, R. Georgii, C. Pfleiderer, and P. Böni, Appl. Phys. Lett. **105**, 123505 (2014).
[43]P. K. Willendrup, E. Farhi, and K. Lefmann, Physica B **350**, E735 (2004); P. K. Willendrup, E. Farhi, E. Knudsen, U. Filges, and K. Lefmann, J. Neutron Res. **17**, 35–43 (2014); See www.mcstas.org for information about the ray-tracing simulation package McStas: documentation, tutorial, download of components, support and updated publication database.
[44]See supplementary material at http://dx.doi.org/10.1063/1.4938071 for details about the bending concept, the functional shape of the supermirror walls, the reliability of the bending algorithm, and the consistency-check of the production protocol.
[45]R. G. Valicu, Ph.D. thesis, Technische Universität München, 2012.
[46]C. C. Yuan, F. Yang, F. Kargl, D. Holland-Moritz, G. G. Simeoni, and A. Meyer, Phys. Rev. B **91**, 214203 (2015).
[47]F. Yang, T. Unruh, and A. Meyer, Eur. Phys. Lett. **107**, 26001 (2014).
[48]F. Yang, D. Holland-Moritz, J. Gegner, P. Heintzmann, F. Kargl, C. C. Yuan, G. G. Simeoni, and A. Meyer, Eur. Phys. Lett. **107**, 46001 (2014).
[49]M. D. Ruiz-Martín, D. Holland-Moritz, F. Yang, C. C. Yuan, G. G. Simeoni, T. Hansen, U. Rütt, O. Gutowski, J. Bednarĉik, and A. Meyer, "Microscopic and macroscopic properties of Zr2Co melts in comparison with those of other binary Zr-based liquids," Phys. Rev. B (submitted).
[50]F. Kargl, H. Weis, T. Unruh, and A. Meyer, J. Phys.: Conf. Ser. **340**, 012077 (2012).
[51]M. Engelhardt, A. Meyer, F. Yang, G. G. Simeoni, and F. Kargl, "Self and chemical diffusion in liquid Al-Ag," Defect Diffus. Forum (to be published).
[52]G. G. Simeoni, "Neutron spectroscopy at high pressure: signal/background discrimination via time-of-flight analysis" (unpublished).
[53]D. D. DiJulio, E. Lelièvre-Berna, P. Courtois, K. H. Andersen, and P. M. Bentley, J. Phys.: Conf. Ser. **528**, 012006 (2014).